

SUPPORTING INFORMATION

Tunable Prussian blue analogues for the selective synthesis of propargylamines through A^3 coupling

Carlos Marquez, Francisco G. Cirujano, Cédric Van Goethem, Ivo Vankelecom, Dirk De Vos*, and Trees De Baerdemaeker*

Centre for Surface Chemistry and Catalysis, KU Leuven, Celestijnenlaan 200F, 3001 Leuven, Belgium.

*Corresponding authors: dirk.devos@kuleuven.be; trees.debaerdemaeker@kuleuven.be.

Table of content

Synthesis of PBAs	S2
Synthesis of multi-metal Cu_xZn_{1-x} -Co PBA	S2
Characterization of the PBAs	S2
A^3 coupling reaction procedure	S3
Table S1. Elemental analysis of selected PBA samples	S4
Figure S1. PXRD patterns of the bimetallic PBA samples	S4
Figure S2. FTIR spectra of the bimetallic PBA samples	S5
Table S2. Textural properties and Lewis acidity of the PBA samples	S5
Figure S3. Nitrogen physisorption isotherms of PBA samples	S6
Figure S4. Difference IR spectra of adsorbed pyridine of selected PBA samples	S6
Figure S5. Yield to the A^3 product over PBAs	S7
Figure S6. Productivity for the A^3 coupling and MPV reduction over Fe-Co PBA	S7
Figure S7. Selectivity to the A^3 product at different phenylacetylene conversions	S8
Figure S8. Pawley refinement of $Cu_{0.86}Zn_{0.14}$ -Co PBA	S8
Figure S9. Pawley refinement of Cu-Co PBA	S9
Figure S10. Pawley refinement of Zn-Co PBA	S9
Table S3. Crystallographic parameters obtained from the Pawley refinement	S10
Figure S11. PXRD patterns of the multi-metal PBA samples	S10
Figure S12. FTIR spectra of the multi-metal PBA samples	S11
Table S4. Comparison of PBAs with homogeneous and heterogeneous catalysts from literature	S11
Table S5. Yield of the A^3 coupling product over $Cu_{0.86}Zn_{0.14}$ -Co PBA using different solvents	S12
Figure S13. Yield vs. time plot for the A^3 coupling reaction over $Cu_{0.86}Zn_{0.14}$ -Co PBA	S12
Figure S14. Relation between the concentration of phenylacetylene and time	S13
Figure S15. Reaction rate vs. the concentration of phenylacetylene	S13
Figure S16. Reaction rate vs. the concentration of piperidine	S14
Figure S17. Hot filtration test	S14
Figure S18. PXRD patterns of $Cu_{0.86}Zn_{0.14}$ -Co PBA after one reaction cycle	S15
Figure S19. FTIR spectra of $Cu_{0.86}Zn_{0.14}$ -Co PBA after one reaction cycle	S15
References	S16

Experimental

Synthesis of PBAs

A series of PBAs were synthesized following previously reported procedures [1,2]. In short, 15 ml of a 0.1 M aqueous solution of $K_3[Co(CN)_6]$ was added dropwise, under continuous stirring, to 150 ml of a 0.1 M aqueous solution of a $M^I Cl_2 \cdot xH_2O$ salt ($FeCl_2 \cdot 4H_2O$, $CoCl_2$, $NiCl_2 \cdot 6H_2O$, $CuCl_2 \cdot 2H_2O$ or $ZnCl_2$) containing 1.5 mmol of poly(tetramethylene ether) glycol (PTMEG). After both solutions were mixed, 37.5 ml of *tert*-butanol ($tBuOH$) was added and the mixture was stirred for 3 h at room temperature. The precipitate was recovered by centrifugation, washed three times with 50 ml of a 50 : 50 mixture of water : $tBuOH$ and dried at 333 K overnight. The solids Fe-Co, Co-Co, Ni-Co, Cu-Co and Zn-Co PBA were obtained using the respective M^I sources.

Synthesis of multi-metal Cu_xZn_{1-x} -Co PBAs

A series of multi-metal complexes, Cu_xZn_{1-x} -Co PBAs, were obtained by tuning the initial synthesis molar ratio of $CuCl_2 \cdot 2H_2O$ and $ZnCl_2$. Briefly, an aqueous solution of $K_3[Co(CN)_6]$ (0.1 M, 15 ml) was added dropwise, under continuous stirring, to another aqueous solution (150 ml) containing 1.5 mmol of PTMEG and specific amounts of $CuCl_2 \cdot 2H_2O$ and $ZnCl_2$ (15 mmol in total). Then, 37.5 mL of $tBuOH$ were added and the mixture was stirred for 3 h at room temperature. The precipitate was recovered by centrifugation, washed three times with a 50 : 50 mixture of water : $tBuOH$ and dried at 333 K overnight.

Characterization

ICP-OES analyses were used to determine the metal content of the catalysts using a Varian 720-ES equipped with a double-pass glass cyclonic spray chamber, a Sea Spray concentric glass nebulizer and a high solids torch. The digestion of the samples was done following a previously reported procedure [3]. PXRD patterns were collected over a $5-60^\circ 2\theta$ range on a STOE Stadi MP diffractometer (in transmission mode) using an image plate detector and focusing $Ge(111)$ monochromator ($CuK\alpha_1$ radiation, $\lambda = 1.54060 \text{ \AA}$). Additional high resolution PXRD patterns for the samples Cu-Co, Zn-Co and $CuZn$ -Co PBA were collected at the I11 beamline (Diamond Light Source, Oxfordshire, UK) using the Mythen2 PSD detector over the range $2-92^\circ 2\theta$. The wavelength of the radiation was obtained by refining a Si NIST

640c standard. Prior to measurements, the samples were finely ground and loaded into borosilicate capillaries (0.5 mm diameter). Pawley refinements of these powder diffraction patterns were performed using the TOPAS-Academic structure refinement software (version 5) [4,5]. N₂ physisorption isotherms were collected at 77 K on a Micromeritics 3Flex Surface Analyzer. The specific surface area (S_{BET}) was determined using the BET method (0.05 – 0.3 p/p_0 range) and the specific external surface area (S_{ext}) and micropore volume (V_{micro}) were obtained using t -plot analysis. Before analyses the samples were after evacuated at 423 K for 16 h. FTIR spectra of KBr wafers (1 wt.% of sample) were collected on a Bruker IFS 66 v/S Vacuum FTIR spectrometer. The acid nature and acid site density were determined by pyridine adsorption followed by FTIR spectroscopy (Py-FTIR) using a Nicolet 6700 FTIR spectrometer. To this end, a self-supporting wafer ($\sim 10 \text{ mg}\cdot\text{cm}^{-2}$) was placed in a cell under vacuum and activated at 523 K for 1 h. The cell was then cooled down and the probe molecule was adsorbed onto the wafer at 323 K until saturation (25 mbar). The physisorbed and excess pyridine were removed by evacuation for 30 min before reheating to 423 K to record the IR spectrum. The acid site density was calculated from the areas of the absorption bands around 1450 cm^{-1} , which correspond to pyridine coordinated to Lewis acid sites and using the integrated molar extinction coefficient from Emeis [6]. High angle annular dark field (HAADF) images and EDX maps were obtained in a JEOL ARM-200F TEM with a probe Cs corrector operated at 200 kV. Prior to imaging, the samples were suspended in ethanol and dropped onto a Cu grid (300 Mesh, Pacific Grid Tech, USA) coated with a Lacey carbon layer.

A³ coupling reaction

Prior to reaction, the catalyst was activated at 353 K under vacuum overnight. Glass crimp cap reaction vials were loaded with 10 mg of the catalyst, phenylacetylene (0.05 mmol), piperidine (0.1 mmol), benzaldehyde (0.1 mmol), 2-butanol (0.5 ml) as solvent (unless otherwise specified) and dodecane (0.1 mmol) as internal standard. The vials were placed in a heated copper block at 383 K and stirred at 500 rpm using a magnetic stirring bar. After reaction, the catalyst was removed by centrifugation and the liquid supernatant was analyzed by GC (Shimadzu 2014 GC equipped with a FID detector and a CP-Sil 5 CB column) and GC-MS (Agilent 6890 gas chromatograph, equipped with a HP-5MS column, coupled to a 5973 MSD mass spectrometer). Recycling test reactions were carried out after recovery and re-activation of the sample before each run. Further reactions varying the initial concentration of phenylacetylene and piperidine were carried out in order to assess the kinetics of the reaction.

Moreover, the effect of the solvent was studied by repeating the reaction using toluene, dioxane and DMSO (dimethyl sulfoxide) as solvents.

Table S1. Elemental analysis of selected PBA samples.

PBA	Cu/Zn _{initial} ^a	Cu (wt.%)	Zn (wt.%)	Co (wt.%)	M ¹ /Co ^b	Cu/Zn _{PBA} ^c
Zn-Co	-	-	31.3	19.0	1.80	-
Cu _{0.14} Zn _{0.86} -Co	0.05	5.8	28.8	17.9	1.74 ^d	0.17
Cu _{0.26} Zn _{0.74} -Co	0.10	9.5	24.9	18.0	1.72 ^d	0.35
Cu _{0.41} Zn _{0.59} -Co	0.15	15.0	21.3	17.4	1.89 ^d	0.71
Cu _{0.67} Zn _{0.33} -Co	0.3	23.5	12.6	17.5	1.90 ^d	2.0
Cu _{0.86} Zn _{0.14} -Co	1.0	30.8	5.8	17.3	1.98 ^d	6.0
Cu _{0.86} Zn _{0.14} -Co ^e	1.0	30.8	5.8	17.3	1.98 ^d	6.0
Cu _{0.96} Zn _{0.04} -Co	9.0	32.9	1.5	18.0	1.77 ^d	25.5
Cu-Co	-	30.7	-	19.0	1.60	-

^a Initial CuCl₂·2H₂O : ZnCl₂ molar ratios used during synthesis. ^b Molar ratios determined by ICP. ^c Cu/Zn molar ratios in the multi-metal PBA complex determined by ICP. ^d (Cu+Zn)/Co molar ratio. ^e Elemental analysis after one reaction cycle.

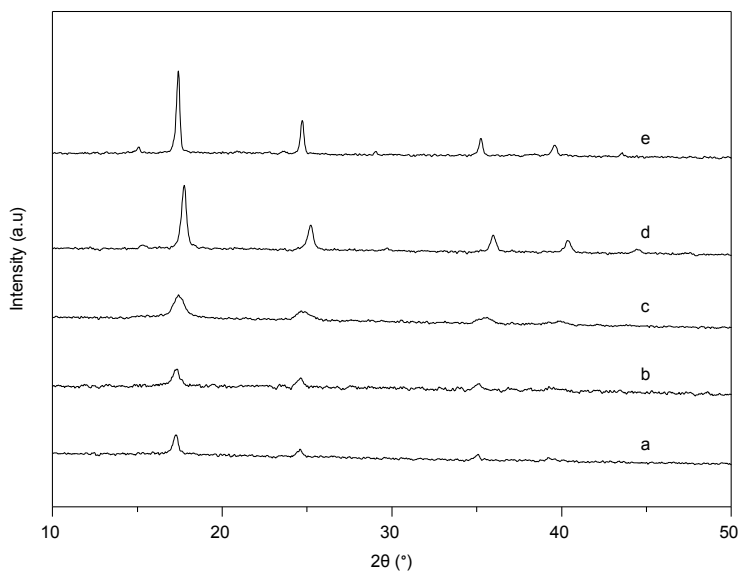


Fig. S1. PXRD patterns for PBA samples: a) Fe-Co, b) Co-Co, c) Ni-Co, d) Cu-Co and e) Zn-Co.

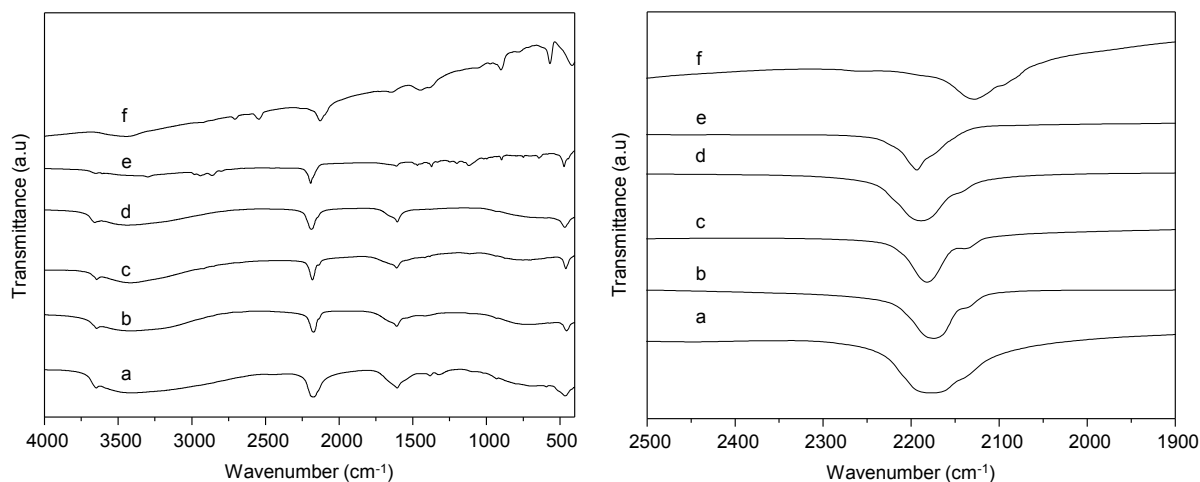


Fig. S2. FTIR spectra (left) and C≡N stretching region of the FTIR spectra (right) of: (a) Fe-Co PBA, (b) Co-Co PBA, (c) Ni-Co PBA, (d) Cu-Co PBA, (e) Zn-Co PBA and (f) $K_3Co(CN)_6$.

Table S2. Textural properties of the PBA samples determined from N_2 physisorption at 77 K and Lewis acid properties determined by pyridine adsorption followed by FTIR spectroscopy.

PBA	S_{BET} (m ² /g)	S_{ext} (m ² /g)	V_{micro} (cm ³ /g)	LAS (mmol/g) ^a
Fe-Co	641	311	0.168	-
Co-Co	1076	327	0.382	-
Ni-Co	114	39	0.038	-
Cu-Co	540	147	0.201	0.044
$Cu_{0.86}Zn_{0.14}$ -Co	567	147	0.222	0.053
Zn-Co	666	138	0.270	0.073

^a Amount of pyridine adsorbed on Lewis acid sites (LAS) per gram of PBA. IR spectra recorded at 423 K.

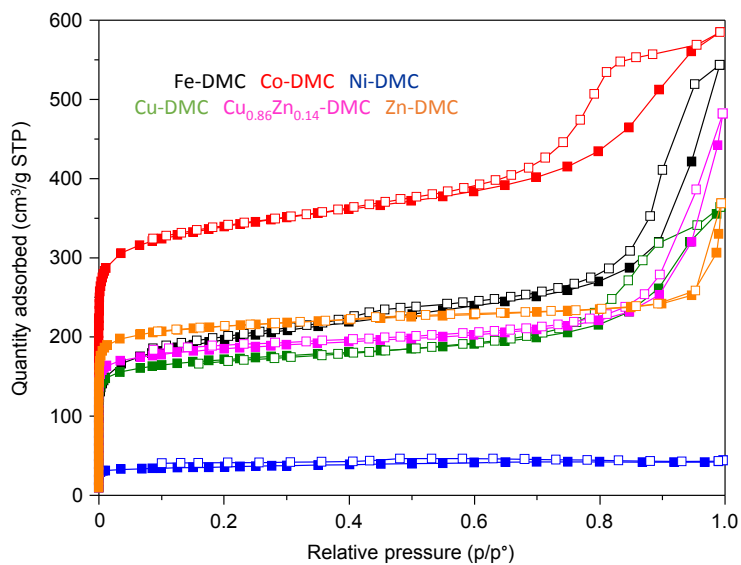


Fig. S3. Nitrogen physisorption isotherms of PBA samples. Filled symbols denote adsorption and open symbols denote desorption.

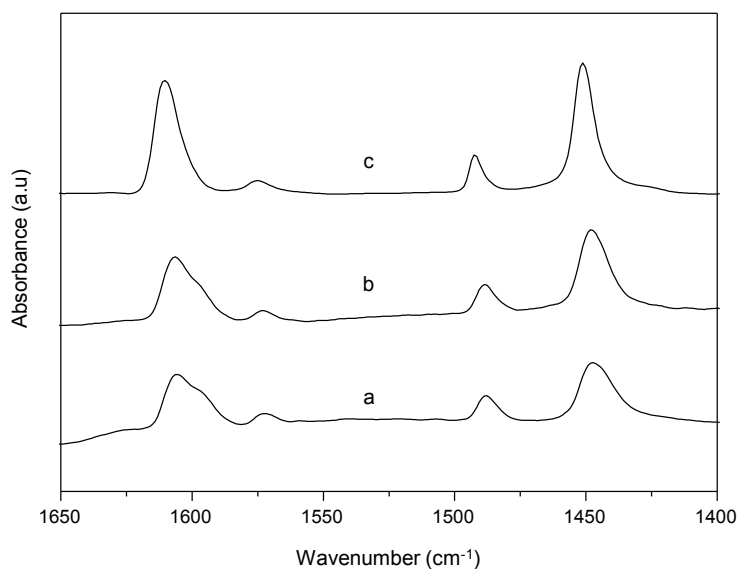


Figure S4. Difference IR spectra of adsorbed pyridine (normalized to 10 mg of PBA/cm²) for:
 a) Cu-Co PBA b) Cu_{0.86}Zn_{0.14}-Co PBA and c) Zn-Co PBA.

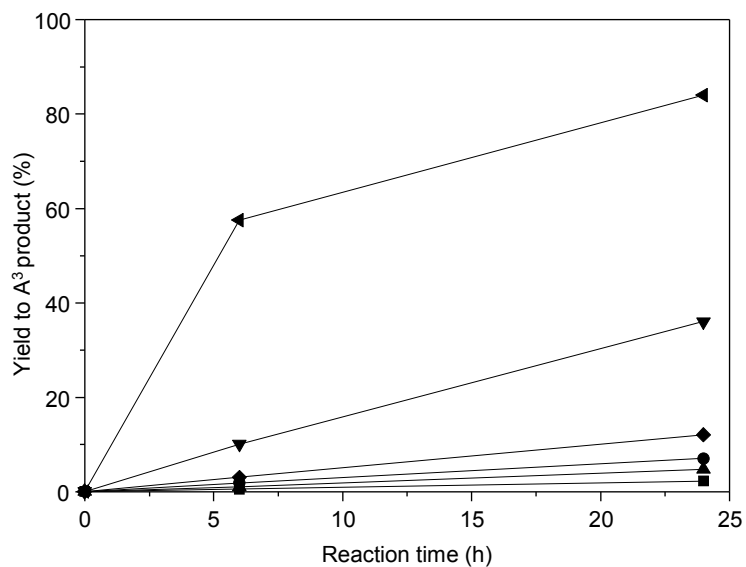


Fig. S5. Yield to the A³ product in the coupling of phenylacetylene (0.05 mmol), piperidine (0.1 mmol) and benzaldehyde (0.1 mmol) at 383 K over PBAs: Fe-Co (■), Co-Co (●), Ni-Co (▲), Cu-Co (▼), Zn-Co (◆), Cu_{0.86}Zn_{0.14}-Co (◄).

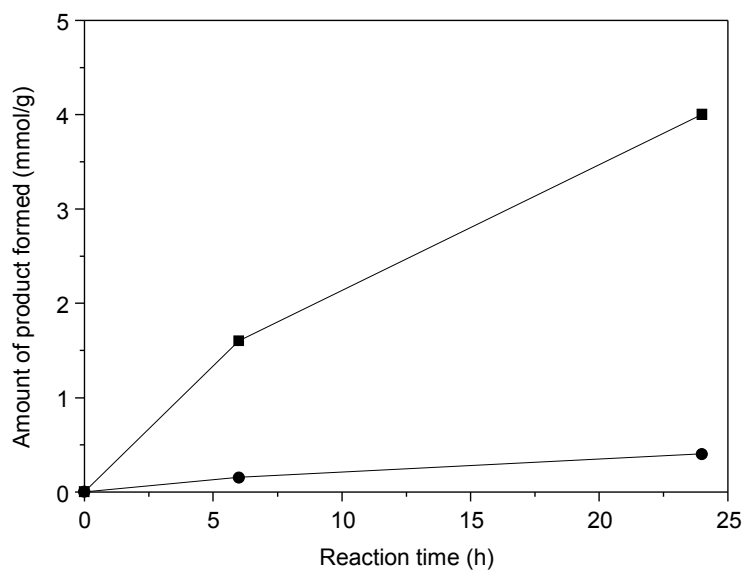


Fig S6. Productivity for the A³ coupling (●) and MPV reduction (■) reaction expressed as mmol of product (A³ product and benzyl alcohol, respectively) formed per g of Fe-Co PBA.

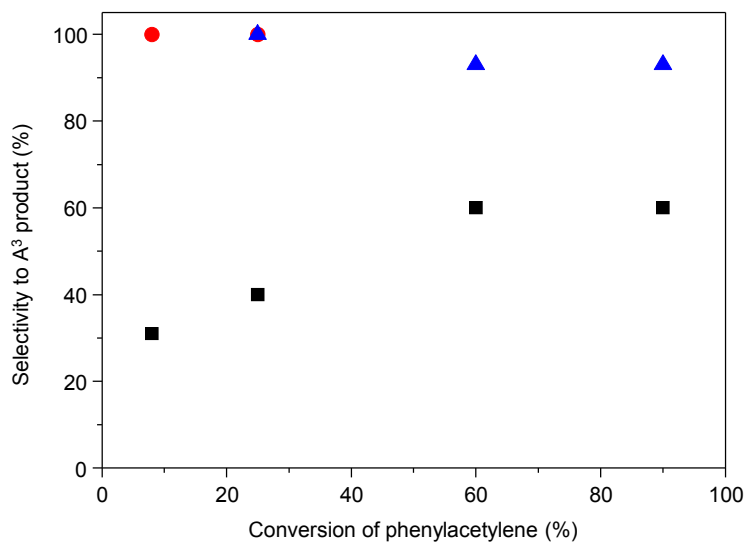


Fig. S7. Selectivity to the A³ product at different phenylacetylene conversions with Cu-Co PBA (■), Zn-Co PBA (●) and Cu_{0.86}Zn_{0.14}-Co PBA (▲).

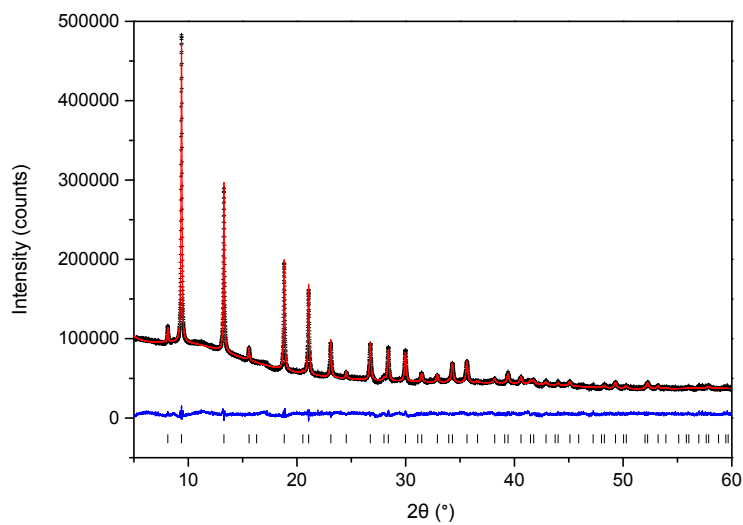


Fig. S8. Pawley refinement of Cu_{0.86}Zn_{0.14}-Co PBA: observed pattern (+), calculated pattern (red line), difference (blue line) and expected peak positions (|).

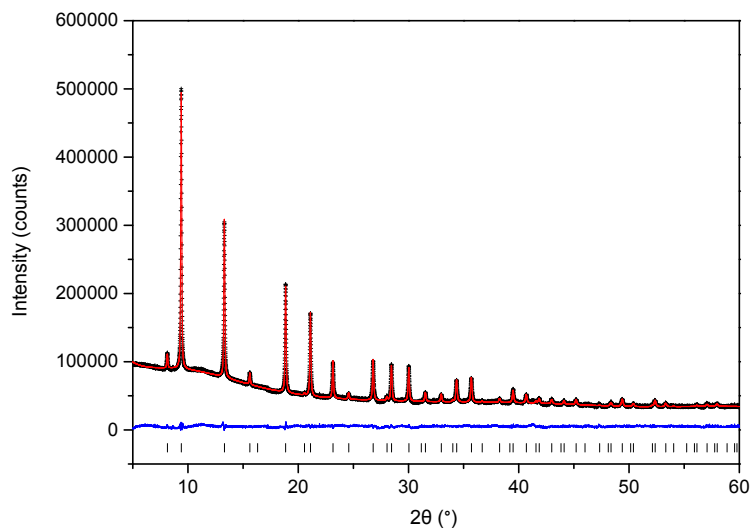


Fig. S9. Pawley refinement of Cu-Co PBA: observed pattern (+), calculated pattern (red line), difference (blue line) and expected peak positions (|).

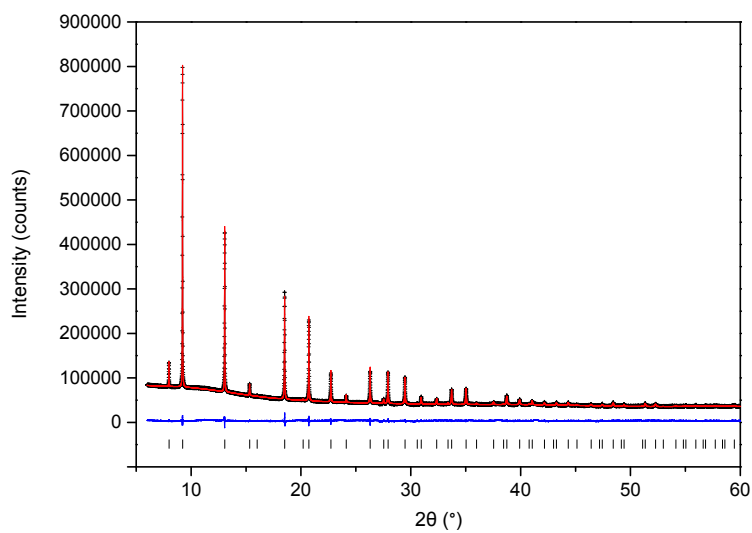


Fig. S10. Pawley refinement of Zn-Co PBA: observed pattern (+), calculated pattern (red line), difference (blue line) and expected peak positions (|).

Table S3. Summary of the crystallographic parameters obtained from the Pawley refinement of selected PBA samples.

	Cu-Co	Zn-Co	Cu _{0.86} Zn _{0.14} -Co
Wavelength (Å)	0.82522	0.82538	0.82522
Space group	<i>Fm-3m</i>	<i>Fm-3m</i>	<i>Fm-3m</i>
<i>a</i> (Å)	10.07163 (18)	10.26025 (17)	10.0908 (3)
<i>R</i> _{wp} (%)	3.05	2.98	3.10
χ^2	32.1	25.3	37.2

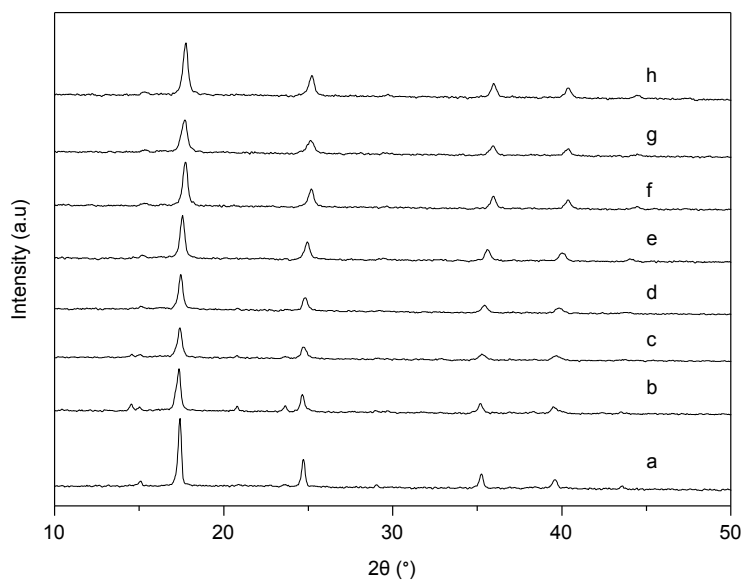


Fig. S11. PXRD patterns for PBA samples: a) Zn-Co, b) Cu_{0.14}Zn_{0.86}-Co, c) Cu_{0.26}Zn_{0.74}-Co, d) Cu_{0.41}Zn_{0.59}-Co, e) Cu_{0.67}Zn_{0.33}-Co, f) Cu_{0.86}Zn_{0.14}-Co, g) Cu_{0.96}Zn_{0.04}-Co and h) Cu-Co.

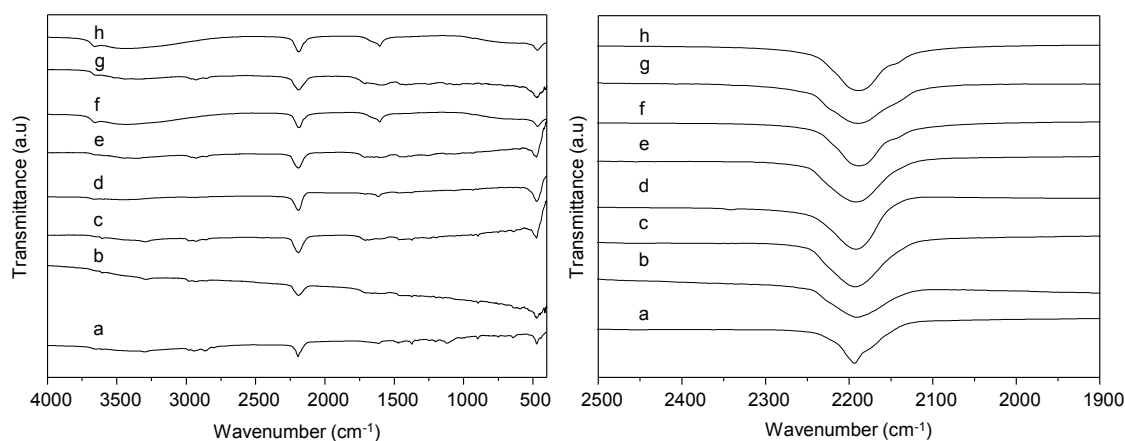


Fig. S12. FTIR spectra (left) and C≡N stretching region of the FTIR spectra (right) of: a) Zn-Co, b) Cu_{0.14}Zn_{0.86}-Co, c) Cu_{0.26}Zn_{0.74}-Co, d) Cu_{0.41}Zn_{0.59}-Co, e) Cu_{0.67}Zn_{0.33}-Co, f) Cu_{0.86}Zn_{0.14}-Co, g) Cu_{0.96}Zn_{0.04}-Co and h) Cu-Co.

Table S4. Comparison of PBAs with homogenous catalysts and heterogeneous catalyst from literature.

Catalyst	6 h		24 h	
	X (%) ^a	Y A ³ (%) ^b	X (%) ^a	Y A ³ (%) ^b
Zn-Co PBA	3	3	12	12
Cu-Co PBA	25	10 ^c	60	36 ^c
Cu _{0.86} Zn _{0.14} -Co PBA	60	56 ^c	90	85 ^c
Cu(OAc) ₂	97	4 ^d	>99	5 ^d
Cu(ClO ₄) ₂	69	<1 ^d	90	<1 ^d
CuCl ₂	94	<1 ^d	>99	<1 ^d
ZnCl ₂	35	33 ^c	70	66 ^c
[Cu(2-pymo) ₂]	-	-	-	71 ^e
CuNPs/G	-	-	-	96 ^f

^a Conversion of phenylacetylene. ^b Yield of the A³ product based on phenylacetylene. ^c Acetophenone was the only side-product detected. ^d 1,4-diphenylbuta-1,3-diyne (from the homocoupling of phenylacetylene) was the only side-product detected. ^e Yield after 21 h. Reaction conditions: 1 mmol phenylacetylene, 1.1 mmol benzaldehyde, 1.1 mmol piperidine, 1 mL dioxane, 10%mol Cu, 373 K (N₂ atmosphere) [7]. ^fYield after 24 h. Reaction conditions: 1 mmol of phenylacetylene, 1.2 mmol of benzaldehyde, 1.2 mmol of piperidine, 3 ml of toluene, 1 mol% Cu/G (2.6 wt%), 373 K (N₂ atmosphere) [8].

Table S5. Yield (%) of the A³ coupling product at 383 K over Cu_{0.86}Zn_{0.14}-Co PBA using different solvents.

Reaction time (h)	Solvent			
	2-Butanol	Dioxane	Toluene	DMSO
6	54	5	3	4
24	85	14	6	10

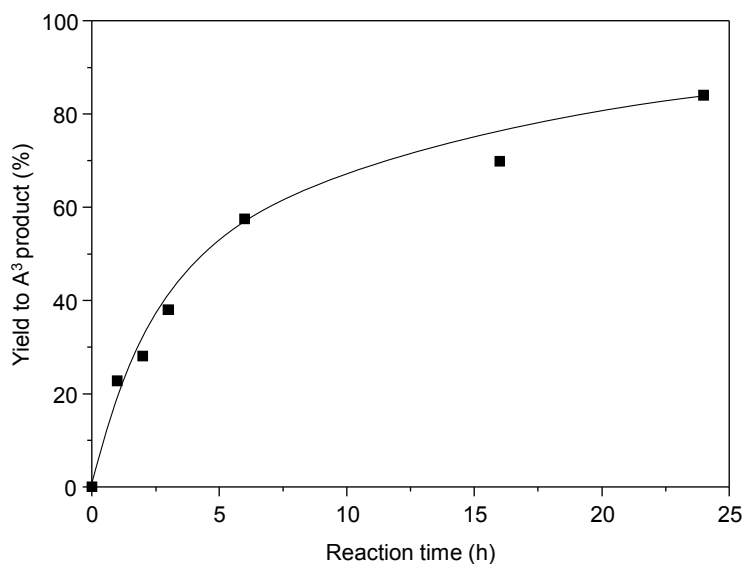


Fig. S13. Yield to A³ product vs. time plot for the coupling of phenylacetylene (0.05 mmol), piperidine (0.1 mmol) and benzaldehyde (0.1 mmol) at 383 K over Cu_{0.86}Zn_{0.14}-Co PBA.

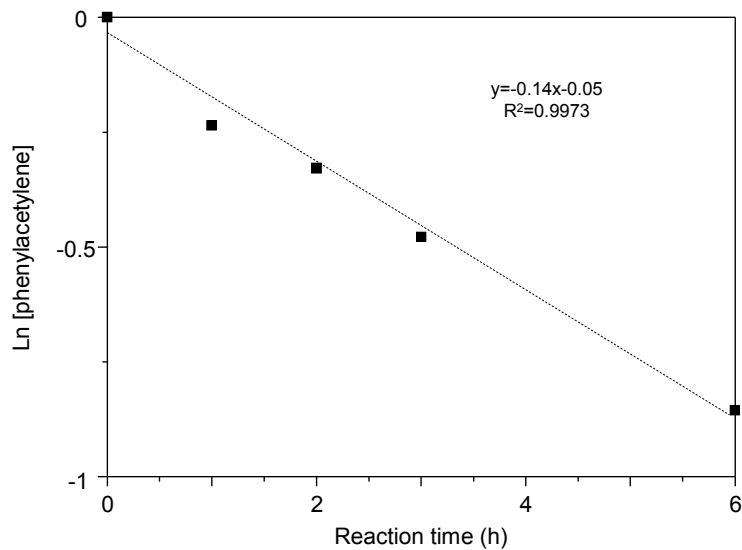


Fig. S14. Linear relation between the natural logarithm of the concentration of phenylacetylene and time. Reaction conditions: phenylacetylene (0.05 mmol), piperidine (0.1 mmol) and benzaldehyde (0.1 mmol) at 383 K over $\text{Cu}_{0.86}\text{Zn}_{0.14}\text{-Co PBA}$.

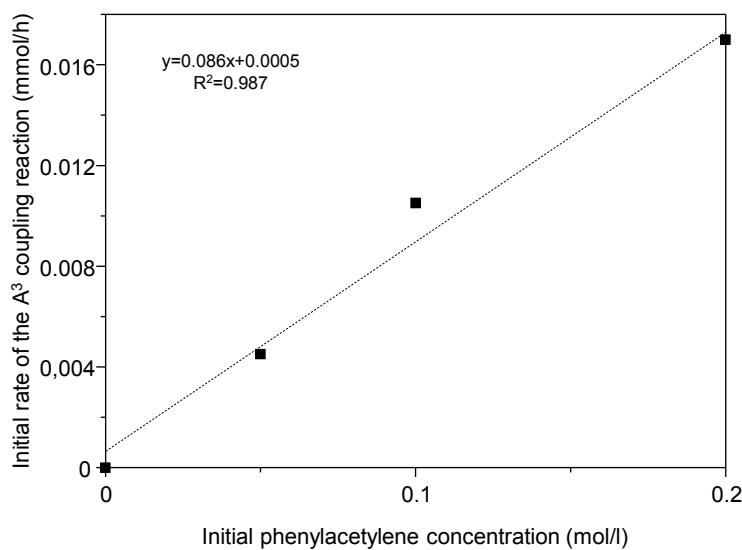


Fig. S15. Variation of the reaction rate with respect to the concentration of phenylacetylene. Reactions were carried out with 0.1 mmol of piperidine and 0.1 mmol of benzaldehyde at 383 K for 1 h over $\text{Cu}_{0.86}\text{Zn}_{0.14}\text{-Co PBA}$.

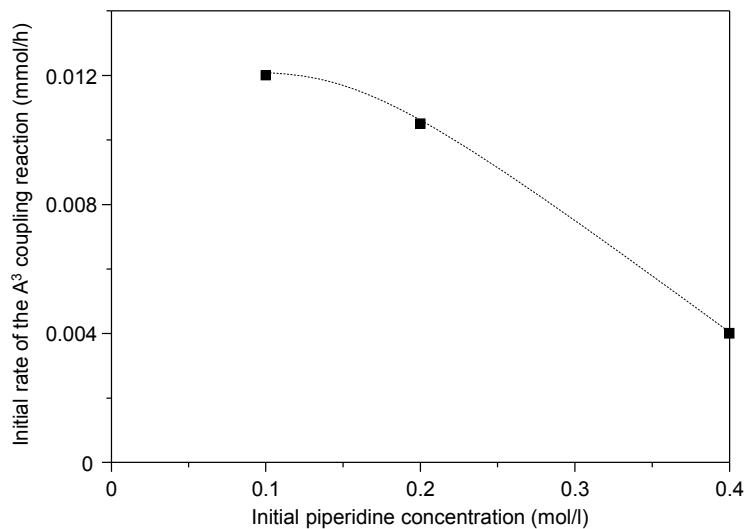


Fig. S16. Variation of the reaction rate with respect to the concentration of piperidine. Reactions were carried out with 0.05 mmol of phenylacetylene and 0.1 mmol of benzaldehyde at 383 K for 1 h over $\text{Cu}_{0.86}\text{Zn}_{0.14}\text{-Co PBA}$.

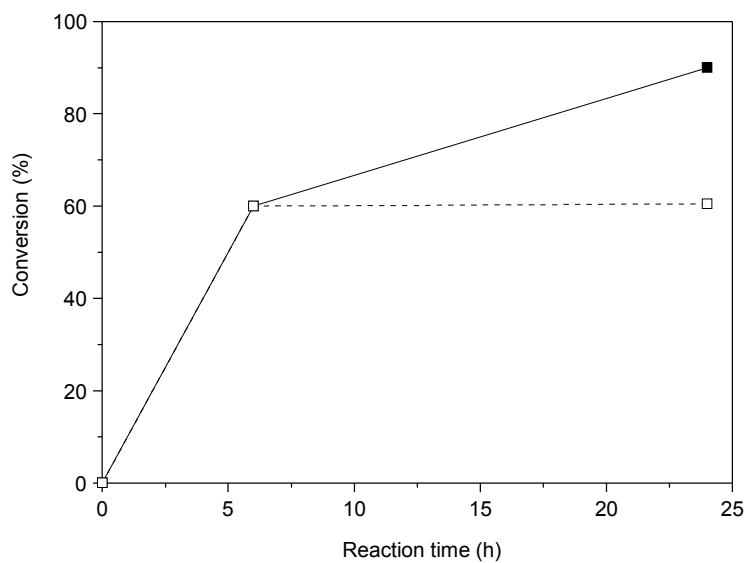


Fig. S17. Conversion of phenylacetylene in the A³ coupling of phenylacetylene (0.05 mmol), piperidine (0.1 mmol) and benzaldehyde (0.1 mmol) at 383 K over $\text{Cu}_{0.86}\text{Zn}_{0.14}\text{-Co PBA}$. Dashed lines represent the conversion after removal of the catalyst in the hot filtration test.

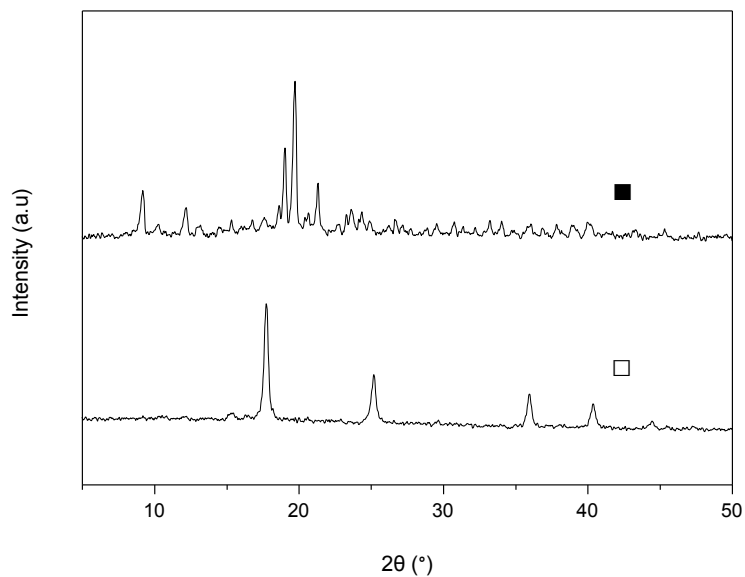


Fig. S14. XRD pattern of $\text{Cu}_{0.86}\text{Zn}_{0.14}\text{-Co PBA}$ before (□) and after (■) the A^3 coupling reaction. Reaction conditions: phenylacetylene (0.05 mmol), piperidine (0.1 mmol) and benzaldehyde (0.1 mmol). 24 h at 383 K.

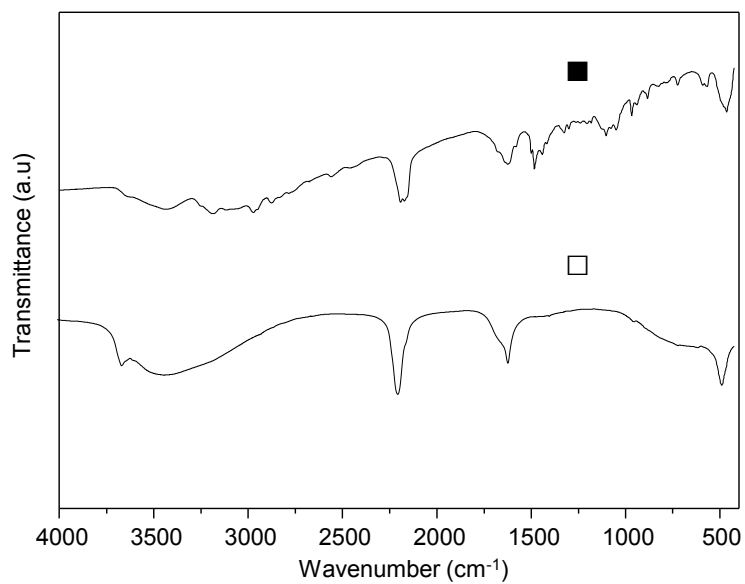


Fig. S15. FTIR spectrum of $\text{Cu}_{0.86}\text{Zn}_{0.14}\text{-Co PBA}$ before (□) and after (■) the A^3 coupling reaction. Reaction conditions: phenylacetylene (0.05 mmol), piperidine (0.1 mmol) and benzaldehyde (0.1 mmol). 24 h at 383 K.

References

- [1] Marquez, C.; Rivera-Torrente, M.; Paalanen, P. P.; Weckhuysen, B. M.; Cirujano, F. G.; De Vos, D.; De Baerdemaeker, T. *J. Catal.* **2017**, 354, 92-99.
- [2] Kim, I.; Ahn, J. T.; Ha, C-S.; Yang, C. S.; Park, I. *Polymer* **2003**, 44, 3417-3428.
- [3] Lee, Y.; Kim, S.; Kang, J. K.; Cohen, S. M. *Chem. Commun.* **2015**, 51, 5735-5738.
- [4] Pawley, G. S. *J. Appl. Crystallogr.* **1981**, 14, 357-361.
- [5] Coelho, A. TOPAS-Academic: General Profile and Structure Analysis Software for Powder Diffraction Data, version 4.1; Coelho Software: Brisbane, Australia, 2007.
- [6] Emeis, C. A. *J. Catal.* **1993**, 141, 347-354.
- [7] Luz, I.; Llabrés i Xamena, F. X.; Corma, A. *J. Catal.* **2012**, 285, 285–291.
- [8] Frindy, S.; El Kadib, A.; Lahcini, M.; Primo, A.; García, H. *Catal. Sci. Technol.* **2016**, 6, 4306–4317.